

# Segmentation of Cerebral Lobes in 3.0 T IR-FSPGR MR Images Using Fuzzy Inference

Yuji Fujiki, Syoji Kobashi<sup>1</sup>, Mieko Matsui<sup>2</sup>, Noriko Inoue<sup>2</sup>, Katsuya Kondo<sup>1</sup>,  
Yutaka Hata<sup>1</sup>, and Tohru Sawada<sup>2</sup>

<sup>1</sup>Graduate School of Engineering,  
Himeji Institute of Technology,  
2167, Shosha, Himeji, 671-2201, Japan

<sup>2</sup>BF Research Institute, Inc.,  
c/o National Cardiovascular Center,  
5-7-1, Fujishirodai, Suita, Osaka 565-0873, Japan

fujiki@comp.eng.himeji-tech.ac.jp

## Abstract

*This paper proposes a computer-aided system for segmenting the frontal, parietal, temporal, and occipital lobes from 3-D human brain 3.0 T IR-FSPGR MR images. Because there is no conventional definition about the cerebral lobes inside the cerebrum, the first work of this research is to define the cerebral lobes using anatomical landmarks, which are the central sulcus, Sylvian fissure, parieto-occipital sulcus, and anterior and posterior commissures. The proposed system finds the boundary by using a fuzzy rule-based active contour model with respect to the anatomical landmarks. For investigating the ability of the reproducibility of the proposed system, MR images of three healthy subjects were analyzed by three beginners and one expert using the proposed system. Each operator segmented ten times per one serial dataset for each subject. Experimental results showed that the system segmented the cerebral lobes with high reproducibility for any subjects and any users.*

## 1. Introduction

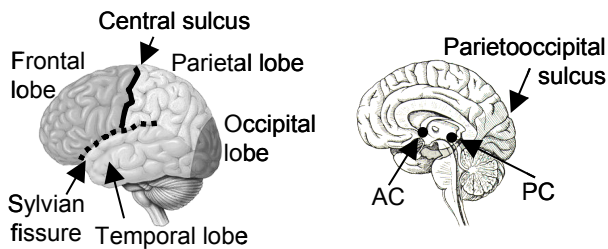
Diffuse brain atrophy is observed across the whole cerebrum as the progress of dementia such as the Alzheimer's disease (AD) and the frontotemporal dementia (FTD), but the atrophy doesn't occur at the same rate across the cerebrum [1][2]. The medial temporal and parietal lobes, for example, atrophy mainly in early stage of AD. In FTD, atrophy is particularly severe around the frontal lobe and the temporal tip. To quantitatively validate the difference of the rate of atrophy across the cerebrum, we should measure the volume and surface area of each cerebral lobe.

The cerebrum is composed of the frontal, parietal, temporal, and occipital lobes. Generally, the cerebral

lobes are classified on the cerebral cortex (e.g., [3]). For example, the frontal lobe is surrounded by the Sylvian fissure and the central sulcus. However, we cannot measure the volume and surface area according to the conventional definition of the cerebral lobes because the boundary inside the cerebrum is not defined.

A few approaches to define the cerebral lobes inside the cerebrum have been discussed. Zeng *et al.* defined the cerebral lobes inside the cerebrum [4]. In this definition, the boundary between the parieto-temporal and the occipital lobes is inadequate, because the boundary varies with the subject. In addition, because these definitions were given to manually measure the volume of the cerebral lobes, they are still not enough for designing a computer-aided segmentation method. We also showed a definition of the frontal lobe [5]. However, the other cerebral lobes, which are the parietal lobe, temporal lobe, and occipital lobe, are not discussed.

There are two approaches for segmenting cerebral lobes using three-dimensional (3-D) volumetric data. One is a manual delineation and the other is an automated segmentation. Manual delineation has low reproducibility due to the lack of rules for segmenting lobes, especially inside the cerebrum. Because it is time-consuming and needs much effort, it is impossible to analyze the large numbers of subjects. In contrast, although automated segmentation can analyze the large numbers of subjects with few operators' effort, there are a few studies on segmentation of cerebral lobes. Ref. [6] and [7] showed a method using a statistical parametric mapping (SPM) software. SPM is the commonly used software for analysis of the brain function [8]. They prepare some MRI templates that are labeled manually into four cerebral lobes. The MRI templates are transformed to the subject's brain using a normalization process of SPM. The cerebrums of the subject are segmented into each lobe using the transformed MRI template. Performance of this



(a) Cerebral surface. (b) Interior cerebrum.  
**Figure 1. Anatomical atlas of the cerebrum.**

method depends on the accuracy of normalization by SPM, which often causes estimation errors. We have proposed a method using a fuzzy rule-based active contour model (ACM) and user-given anatomical landmarks [5]. The method could segment the frontal lobe with high reproducibility (variability of the frontal lobe's volume among ten trials for a given dataset is within 0.95 %). However, the method was not applied to segment the parietal lobe, temporal lobe and the occipital lobe.

In this paper, we propose a computer-aided segmentation system of the cerebral lobes in 3.0 T inversion recovery fast spoiled GRASS (IR-FSPGR) MR images using fuzzy rule-based ACM. Our system has original landmarks, which are the central sulcus, Sylvian fissure, parieto-occipital sulcus, anterior commissure (AC) and posterior commissure (PC). For investigating the ability of the reproducibility of the proposed system, MR images of three healthy subjects were analyzed by one expert and three beginners using the proposed system.

## 2. Materials

Two healthy female subjects (Subject 1, and 2, ages  $40.5 \pm 7.8$  years old, mean  $\pm$  SD) and one healthy male subject (Subject 3, 42 years old) were recruited. They all gave informed consent according to the guidelines approved by the local Ethical Committee at the BF Research Institute, Inc.

MRI studies were performed on a 3.0 T Signa LX VH/i Scanner (GE Medical Systems, Milwaukee, WI) with a circularly polarized head coil as both transmitter and receiver. Images were acquired by a coronal 3-D IR-FSPGR with a repetition time (TR) of 10.7 ms, an actual echo time (TE) of 1.9 ms, and an inversion time (TI) of 600 ms. The field of view (FOV) was 220 mm square. The matrix was 256 by 256. Each volume dataset consisted of 124 separated slices whose thickness was 1.5 mm with no gap. Voxel size was  $0.86 \times 0.86 \times 1.5$  mm<sup>3</sup>.

We constructed the MR volume of the brain, which consisted of  $256 \times 256 \times 124$  voxels. In our system, the MR images appeared and were treated as intensity images. The intensity for all voxels of all intracranial structures ranged between 0 and 4095. The acquired datasets were classified into the left and right cerebral hemispheres,

cerebellum, and brain stem by the automated human brain MR image segmentation algorithm [10].

## 3. Definition of the cerebral lobes

The cerebrum consists of the frontal lobe, parietal lobe, temporal lobe, and occipital lobe illustrated in Fig. 1 (a) [3]. Generally, the cerebral lobes are classified on the cerebral cortex. The frontal lobe is segmented by the central sulcus and Sylvian fissure. The parietal and temporal lobes are classified by Sylvian fissure. The central sulcus is the boundary between the frontal and parietal lobes, and the Sylvian fissure is the boundary between the frontoparietal and temporal lobes. However, this classification can be achieved only on the cerebral cortex. That is, there is no index to classify the cerebral lobes inside the cerebrum. In this paper, we define the cerebral lobes using the anatomical landmarks not only on the cerebral surface but also inside the cerebrum.

The frontal lobe is defined to be a region whose section is formed by the union of all line segments composed of the middle point of the AC-PC line and the points on the closed curve derived from the central sulcus and the Sylvian fissure [5]. AC and PC are well-known anatomical points denoted in Fig. 1 (b).

In this paper, the occipital lobe is defined to be a posterior region segmented by a section, which is formed by extending the parieto-occipital sulcus so that the sulcus crosses the longitudinal fissure of cerebrum vertically.

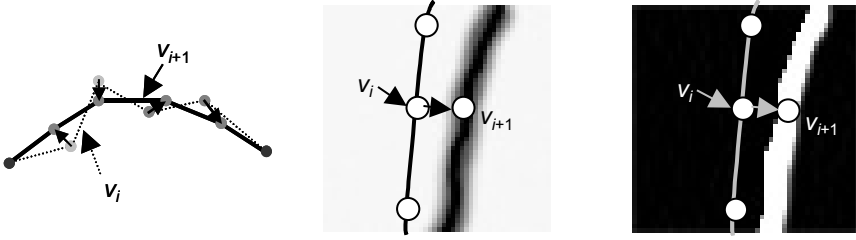
After segmenting the frontal and the occipital lobes from the cerebrum, the remaining region is divided into the parietal lobe and the temporal lobe by using the Sylvian fissure. The boundary is determined by projecting the Sylvian fissure to the longitudinal fissure of cerebrum vertically. Because the posterior tail of the Sylvian fissure is often unclear, the fissure should be extended so that it reaches the parieto-occipital sulcus.

## 4. Segmentation of the cerebral lobes

Segmenting the cerebral lobes is performed with the following four steps:

- 1) Set the anatomical landmarks.
- 2) Segment the frontal lobe [5].
- 3) Segment the occipital lobe.
- 4) Segment the parietal and temporal lobes.

Because the proposed method segments the cerebral lobes according to the anatomical landmarks, which are the central sulcus, the Sylvian fissure, parieto-occipital sulcus, AC and PC, users manually give these landmarks at the first step. To make users easily set the landmarks we have developed a graphical user interface (GUI). The second step segments the frontal lobe by means of the



(a) Feature value  $f_{int}$ . (b) Feature value  $f_{line}$ . (c) Feature value  $f_{edge}$ .

**Figure 2. Feature values.** In (b) and (c), the smaller values of intensity and gradient are appeared as the black.

algorithm described in Ref. [5]. The algorithm uses the AC, PC, central sulcus, and Sylvian fissure as the landmarks for segmentation. Third step generates a section using the parieto-occipital sulcus, and then segments the occipital lobe at the section. Finally, we remove the segmented the frontal and occipital lobes from the cerebrum, and decompose the remaining region into the parietal and temporal lobes according the Sylvian fissure. In the following, we describe the details of the developed GUI, and the algorithms for segmenting the occipital, parietal and temporal lobes.

#### 4.1 Graphical user interface to set the landmarks

Our system runs according to the anatomical landmarks given by users. This enables it to process any data like postoperative/atrophied brains. In this work, we develop a GUI so that users easily set the anatomical landmarks. The GUI consists of two interfaces using a shaded surface display (SSD) and a multi-planar reconstruction (MPR). Using the SSD interface, users can set the 3-D sulcus by drawing lines on the 2-D SSD images. Although sulci are structurally complex, there are some proper angles where users easily recognize them on the cerebral surface. Because these angles vary by user and by subject, the interface should be configured so that the user can select proper angles to recognize the sulci on the SSD image. Using this interface, the Sylvian fissure and the central sulcus are given. The MPR interface consists of three sectional images, which are a coronal, a sagittal, and an axial images. Using this MPR interface, the user can set any point on 3-D space. The AC, PC and the parieto-occipital sulcus are given by using this interface.

#### 4.2 Segmentation of the occipital lobe

We segment the occipital lobe according to the parieto-occipital sulcus given by the user. Because the user-given curves are not set at the deepest point of the parieto-occipital sulcus, our system drops the curves into the deepest point using the fuzzy rule-based ACM (the details are described in the following paragraph). Then the detected parieto-occipital sulcus is extrapolated so that the

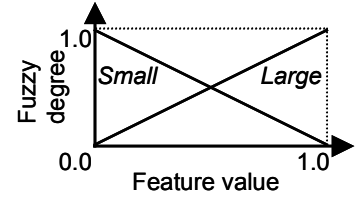


**Figure 3. Membership functions.**

sulcus crosses over the whole cerebrum. The boundary surface of the occipital lobe inside the cerebrum is determined by projecting the extended parieto-occipital sulcus to the longitudinal fissure of cerebrum vertically.

The parieto-occipital sulcus is detected by fitting the user-given curve into the deepest point using the fuzzy rule-based ACM. The fuzzy rule-based ACM, which is proposed in Ref. [5], is a fuzzy logic based extension of the conventional ACM [9]. The principal advantage of the fuzzy rule-based ACM is that it can easily implement physicians' anatomical knowledge with fuzzy if-then rules.

In the fuzzy rule-based ACM, a fitting curve is given by  $v(t) = (z(t), y(t)) (1 \leq t \leq n)$ , where  $n$  is the number of nodes composing the curve. At first, initial nodes of  $v(t)$  are determined by selecting the points at the 2 pixel interval. Then the nodes of the curve are moved so that the curve detects the parieto-occipital sulcus. We then evaluate whether the curve detects the parieto-occipital sulcus or not by estimating a fuzzy degree belonging to the parieto-occipital sulcus. The fuzzy degree is estimated by a mean of fuzzy degrees of every node, and it is given by

$$\mu = \frac{1}{n} \sum_{t=1}^n \mu_t, \quad (1)$$

where  $\mu$  and  $\mu_t$  are fuzzy degrees belonging to the parieto-occipital sulcus for the curve of interest and for node  $t$ , respectively. The fuzzy degree for the node of interest,  $\mu_t$ , is estimated by using knowledge about the parieto-occipital sulcus:

- (1) The parieto-occipital sulcus runs smoothly.
- (2) The parieto-occipital sulcus has low intensity.
- (3) The parieto-occipital sulcus has high gradient of intensity.

To evaluate a node of interest with respect to this knowledge, we define three features of the node,  $f_{int}$ ,  $f_{line}$  and  $f_{edge}$ . The first feature,  $f_{int}$ , estimates the smoothness of the curve at the node of interest, and is given by:

$$f_{int} = \left( \left| \frac{dv(t)}{dt} \right| + \left| \frac{d^2v(t)}{dt^2} \right| \right) / f_{int\_max}. \quad (2)$$

This feature gives the lower value when the node  $v_i$  moves to node  $v_{i+1}$  as shown in Fig. 2 (a). The second

feature,  $f_{line}$ , evaluates the intensity at the node, and is given by:

$$f_{line} = I(x, y) / f_{line\_max} . \quad (3)$$

This feature takes the lower value when the node moves to a voxel with the lower intensity as shown in Fig. 2 (b). The third feature,  $f_{edge}$ , estimates the strength of edge, and is given by:

$$f_{edge} = |\nabla I(x, y)| / f_{edge\_max} , \quad (4)$$

where  $\nabla$  is a gradient operator. This feature gives the lower value when the node moves to a voxel with the higher gradient of intensity as shown in Fig. 2 (c). In the above definitions,  $f_{int\_max}$ ,  $f_{line\_max}$  and  $f_{edge\_max}$  are normalization parameters given by the user. Using these three features, we derive the following two fuzzy IF-THEN rules from the knowledge about the parieto-occipital sulcus:

[Rule 1]

IF ( $f_{int}$  is *Small*) AND ( $f_{line}$  is *Small*) AND  
( $f_{edge}$  is *Large*)  
THEN  $\mu_i$  is *Large*.

[Rule 2]

IF ( $f_{int}$  is *Large*) AND ( $f_{line}$  is *Large*) AND  
( $f_{edge}$  is *Small*)  
THEN  $\mu_i$  is *Small*.

*Small* and *Large* are fuzzy languages defined by membership functions shown in Fig. 3. The fuzzy IF-THEN rules are carried out by a MIN-MAX implementation technique. The consequent fuzzy degree,  $\hat{\mu}_i$ , is the center of gravity of the obtained fuzzy sets. The fuzzy IF-THEN rules are applied to every node, and then the fuzzy degree belonging to the parieto-occipital sulcus of the curve of interest is calculated by Eq. (1) for each node. By iterating with moving nodes so that the fuzzy degree,  $\mu_i$ , is maximized, the parieto-occipital sulcus will be detected.

The detected parieto-occipital sulcus is not still enough for segmenting the occipital lobe because the sulcus does not cross over the whole cerebrum. For example, because the superior tail of the sulcus is often unclear, it is impossible to detect the whole sulcus. Therefore, we extrapolate the detected sulcus so that the sulcus crosses over the whole cerebrum.

Using the obtained parieto-occipital sulcus that completely crosses over the cerebrum from the inferior to the superior, we determine the boundary between the occipital lobe and both the parietal and temporal lobes. According to our definition about the occipital sulcus, the boundary is formed by projecting the obtained parieto-occipital sulcus to the longitudinal fissure of cerebrum vertically. To estimate the longitudinal fissure of cerebrum, we first find the contact points of the right and left cerebral hemispheres by raster scan on axial planes ( $x$ - $z$  plane). Secondly, the contact points are projected on 2-D plane and a line approximating the contacting points is

calculated by using a linear least square method (LSM). Then, the longitudinal fissure of cerebrum is obtained by extending the approximated line for  $y$ -direction. Consequently, a section is obtained by projecting the parieto-occipital sulcus to the longitudinal fissure of cerebrum, and then the occipital lobe is segmented at the obtained section.

### 4.3 Segmentation of the parietal and temporal lobes

The remaining region after removing the frontal lobe and the parietal lobe from the cerebrum is composed of the parietal and temporal lobes. Therefore, the parietal and temporal lobes can be segmented by determining the boundary between them. According to our definition, the boundary is determined by projecting the Sylvian fissure to the longitudinal fissure of cerebrum.

However, because the Sylvian fissure does not reach the parieto-occipital sulcus in almost of cases, we extrapolate the Sylvian fissure so that the sulcus crosses the cerebrum from the anterior to the parieto-occipital sulcus. The extrapolation is done for each cerebral hemisphere separately, and the details are described below. At first, the Sylvian fissure detected by fuzzy rule-based ACM is projected on a 2-D plane. Second, the Sylvian fissure is extrapolated by means of the LSM using a quadratic function on the 2-D projection plane. Third, the extrapolated Sylvian fissure is projected on the 3-D cerebral surface. Finally, we drop the projected Sylvian fissure on the cerebral surface into the deepest point of the sulci by the fuzzy rule-based ACM. The fuzzy IF-THEN rules and conditions are the same as those used to detect the parieto-occipital sulcus.

The boundary between the parietal and temporal lobes are found by projecting the extrapolated Sylvian fissure to the longitudinal fissure of cerebrum, and the parietal and temporal lobes are segmented at the obtained boundary.

## 5. Experimental results and discussion

MR images acquired from Subject 1 were analyzed by the proposed system for demonstrating the ability of segmenting the cerebral lobes. A screenshot of the configured GUI system is shown in Fig. 4. This figure shows a screenshot of the SSD interface. Using this GUI system, a user gave the central sulcus and Sylvian fissure. Then, the user gave the AC and PC points, and the parieto-occipital sulcus using the MPR interface. For running the fuzzy rule-based ACM, three parameters, which are  $f_{int\_max}$ ,  $f_{line\_max}$  and  $f_{edge\_max}$ , were set at 20, 100 and 50, respectively. The same parameters were used across all of our experiments. The computation time for segmentation (not including pre-processing, i.e., segmen-

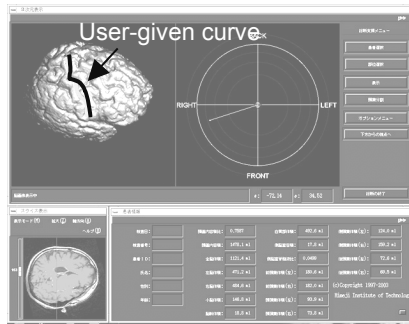


Figure 4. Configured system.

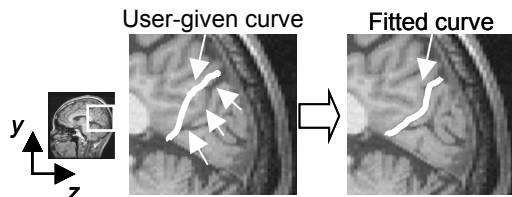
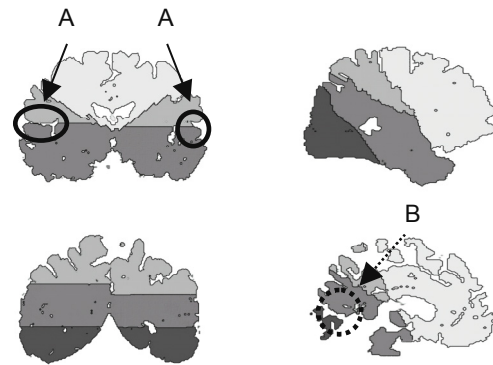


Figure 5. User-given curve is matched to the parieto-occipital sulcus by fuzzy rule-based ACM.

tation of the brain, and decomposing the brain portions) was less than 15 s running on a workstation (Silicon Graphics Fuel™, R14000, 500MHz, 1024MB, SGI). Fig. 5 shows a part of the cerebrum. In this figure, a user-given curve and the fitted curve are described in white solid lines. The user-give curve was fitted at the parieto-occipital sulcus. Coronal and sagittal images of the labeled volume data are shown in Fig. 6. The cerebral lobes were correctly segmented at the proper sulci. In this figure, we can confirm the Sylvian fissure (A) between the parietal and the temporal lobes, and parieto-occipital sulcus (B) between the occipital and the temporal lobes. 3-D SSD images of the segmented cerebral lobes are shown in Fig. 8. These images are visually appropriate compared with Fig. 1 (a). As shown in Fig. 7, the boundaries between the parietal and temporal lobes of the right and left cerebral hemispheres are not same shape because the shape of the Sylvian fissure of the right and left cerebral hemispheres are not same.

We weighed the variability of volumes of cerebral lobes when the system was operated by an expert and three beginners. The expert got well used to our system and could easily detect the central sulcus and Sylvian fissure on the SSD interface, and the parieto-occipital sulcus and the AC and PC points on the MPR interface. Beginners were collected who were not familiar with our system and the location of the anatomical landmarks. Therefore, the beginners were trained on how to use the system about ten minutes, and were instructed on the anatomical landmarks before testing our system. Both of the expert and the three beginners segmented individually ten times per one dataset of the subject.



(a) Coronal images. (b) Sagittal images. Figure 6. The result of segmentation (2-D). (A): the Sylvian fissure, and (B): the parieto-occipital sulcus.

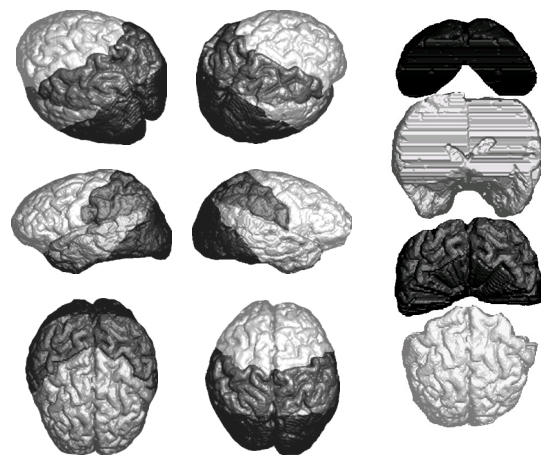
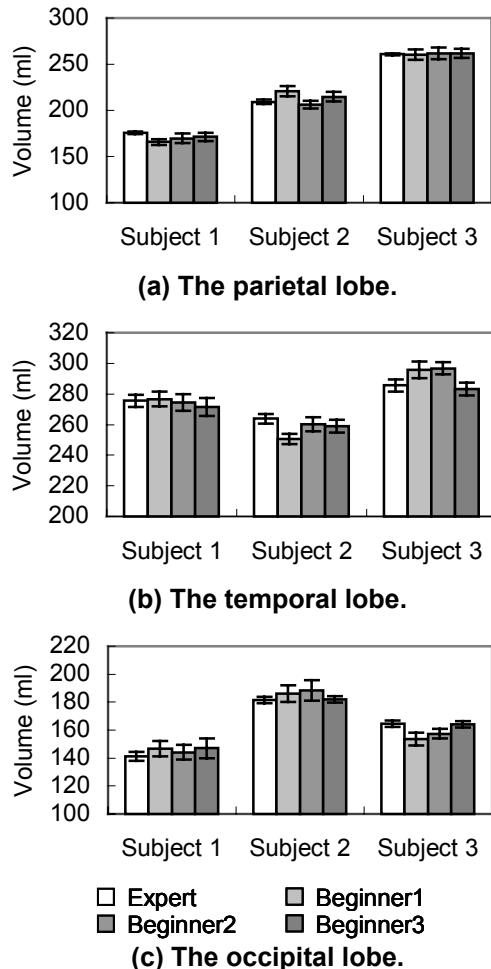


Figure 7. Segmentation results. The cerebrum is segmented into the frontal lobe (light gray), parietal lobe (dark gray), temporal lobe (gray), and occipital lobe (dim gray).

The variabilities of the volumes within a user and across inter users were investigated. Fig. 8 shows mean and SD of volume (block graph) of the cerebral lobes that were segmented by four users. The graphs showed that for any subjects and for all cerebral lobes, (1) the variabilities of the volumes within a user were small, and (2) those across the users relatively were small, however, is larger than those within a user. These results confirmed that by using the proposed system we could segment the cerebral lobes with high reproducibility even if the user is beginner.

## 6. Conclusion

We have proposed a computer-aided system for segmenting the cerebral lobes from 3.0 Tesla IR-FSPGR MR images. To design the system, we first defined the cerebral lobes geometry using the anatomical landmarks. To our knowledge, this will be the first approach to define the cerebral lobes inside the cerebrum.



**Figure 9. Variability of the volumes within a user and among the users.**

The segmentation of the cerebral lobes was performed with the fuzzy rule-based ACM according to the anatomical landmarks, which are given by a user on the SSD and MPR interfaces. The algorithm drops the user-given sulci into the deepest point. This leads the system to produce stable segmentation results. The ability of the reproducibility of the proposed system was evaluated by applying the system to three healthy subjects in which four users operated. The experimental results confirmed that our system could segment the cerebral lobes with high reproducibility even if the user is a beginner, and even if the user differs by each experiment.

There are a few differences between the boundaries segmented by the proposed system and the conventional wisdom at the posterior cerebrum. In the future, we will apply another definition of the occipital lobe so that the system segments the cerebral lobes more stably and more adequately to the conventional wisdom. In addition, a method for automatically detecting the Sylvian fissure and parietooccipital sulcus will be studied.

## Acknowledgments

We thank PhD candidates M. Umeda (Dept. of Medical Informatics, Meiji University of Oriental Medicine) and M. Fukunaga (BF Research Institute, Inc. and Dept. of Medical Informatics, Meiji University of Oriental Medicine) for their advice on MRI. We also thank Mr. S. Itoi (BF Research Instituted. Inc.) for his assistance in MR studies. This work was supported in part by Ministry of Education, Culture, Sports, Science and Technology, Grant-in-Aid for Encouragement of Young Scientists, 15700198, 2003, and the BISC Program of UC Berkeley.

## References

- [1] D. Wang, J. B. Chalk, S. E. Rose, G. Zubizaray, G. Cowin, G. J. Galloway, D. Barnes, D. Spooner, D. M. Doddrell, and J. Semple. MR Image-Based Measurement of Rates of Change in Volumes of Brain Structures. Part II: Application to a Study of Alzheimer's Disease and Normal Aging. *Magn. Reson. Imaging*, 20:41-48, January 2002.
- [2] R. I. Scahill, J. M. Schott, J. M. Stevens, J. M. Rossor, and N. C. Fox. Mapping the Evolution of Regional Atrophy in Alzheimer's Disease: Unbiased Analysis of Fluid-Registered Serial MRI. *Proc. Natl. Acad. Sci.*, 7:4703-4707, 2002.
- [3] H. J. Kretschmann, W. Weinrich. *Klinische Neuroanatomie und Kranielle Bilddiagnostik*. Thieme, 1999.
- [4] X. Zeng, L. H. Staib, R. T. Schultz, and J. S. Duncan. Segmentation and Measurement of the Cortex from 3D MR Images Using Coupled Surfaces Propagation. *IEEE Trans. Med. Imag.*, 18(10):100-111, October 1999.
- [5] Y. Fujiki, S. Kobashi, M. Matsui, N. Inoue, K. Kondo, Y. Hata, and T. Sawada. Interactive 3-D Segmentation of the Frontal Lobe in 3.0T IR-FSPGR MR Images Using Fuzzy Rule-Based ACM. *J. of Advanced Computational Intelligence and Intelligent Informatics*, 7(2):189-199, 2003.
- [6] S. Kanekiyo, H. Toyama, K. Uemura, K. Ishii, and A. Uchiyama. Development of a Method to Divide Brain Lobes Automatically. *Proc. of 40th Japan Soc. ME & Be*, 39:443, 2001. (In Japanese)
- [7] D. L. Collins, N. J. Kabani, and A.C. Evans. Automatic Volume Estimation of Gross Cerebral Structure. *4<sup>th</sup> Int. Conf. on Functional Mapping of the Human Brain*, June 1998.
- [8] K. J. Friston, J. Ashburner, J. B. Poline, C. D. Frith, J. D. Heather, and R. S. J. Frackowiak. Spatial Registration and Normalization of Images. *Human Brain Mapping*, 2:165-189, 1995.
- [9] M. Kass, A. Witkin, and D. Terzopoulou. Snakes: Active Contour Models. *Int. J. of Computer Vision*, 1(4):321-331, 1987.
- [10] Y. Hata, S. Kobashi, S. Hirano, H. Kitagaki, and E. Mori. Automated Segmentation of Human Brain MR Images Aided by Fuzzy Information Granulation and Fuzzy Inference. *IEEE Trans. Syst., Man, Cybern. C*, 30(3):381-395, August 2000.